Bull. Inst. Chem. Res., Kyoto Univ., Vol. 58, No. 1, 1980

Magnetic Field Trimming Effect of Saturated Ferromagnetic Rods

Yoshihisa IWASHITA,* Toshiyasu HIGO,* and Kenro KUROKI**

Received December 7, 1979

A system of magnetic field measurement was constructed to study the trimming effect of saturated ferromagnetic rod. Trim rod method was verified useful to 1% shimming of supersaturated magnetic field.

KEY WORDS: Automatic magnetic field scan / Supersaturated field / Trim rod shimming /

I. INTRODUCTION

Trimming of the magnetic field distribution in the high field superconducting cyclotron is a serious problem. Conventional method which uses trim coils needs very big power consumption and the trimming effect is not yet verified.

A new method fit to the high field (saturated iron) cyclotron was proposed by Bigham of CRNL, which uses an array of iron rods. (see Fig. 1) In this laboratory, we are intending to build a superconducting cyclotron, and as a preparatory work,

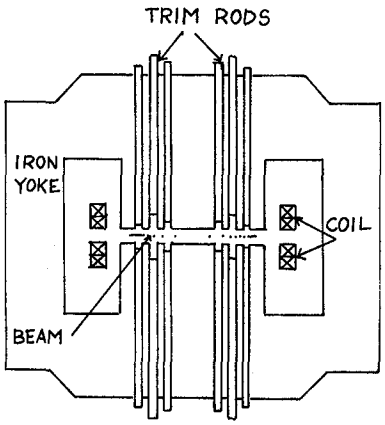

Fig. 1. Superconducting cyclotron cross section indicating the use of trim rods for radial magnetic field trimming.

* 岩下芳久，肥後寿泰: Laboratory of Nuclear Reaction, Institute for Chemical Research, Kyoto University, Kyoto.

** 黒木健郎: Nuclear Science Research Facility, Institute for Chemical Research, Kyoto University, Kyoto.

Present Address; National Research Institute of Police Science, Sanbancho, Chiyodaku, Tokyo.

a small magnet with a trim rod was constructed and the trimming effect was surveyed. The result is very promising.

In this paper, the magnetic shimming effects of the trim rod are described together with the magnetic field profile measuring system.

II. PRINCIPLE OF TRIM ROD

In a high field superconducting cyclotron, the iron poles are saturated magnetically at operating field. This saturation simplifies the field calculation.[1] To calculate the field distribution, it is assumed that the magnetic field is produced by uniformly magnetic-charged surface.

The field perturbation ΔB_1 on the crossing of the axial line of the rod and the median plane is expressed in Eq. (1) as a function of the rod displacement g based on the uniform magnetic charge approximation. In this case, the rod moves as shown in Fig. 2 and the displacement is measured from the surface of the main pole.

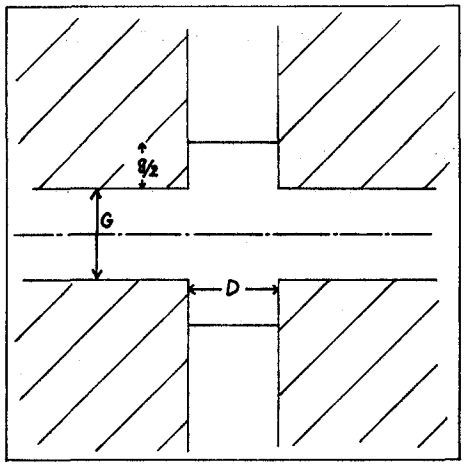

Fig. 2. Radial section of a pair of trim rods. D is the diameter of the rod and G is the gap. $g/2$ is the rod displacement.

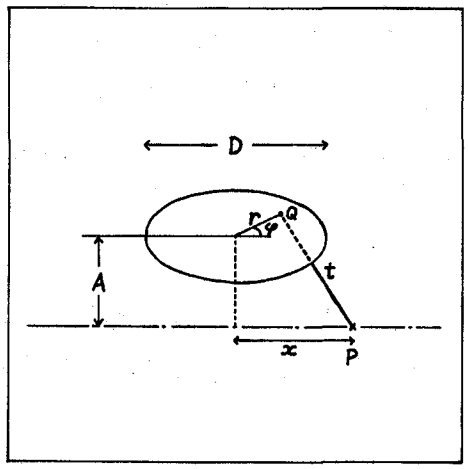

Fig. 3. Coordinate system used in the magnetic field calculation based on uniformly "magnetic-charged" disk model. D is the diameter of disk. A is the distance between the disk and median plane. t is distance between the point Q in the disk and P.

$$\Delta B_1 = \mu_0 M_s \left[\frac{G}{\sqrt{G^2+D^2}} - R \cdot \frac{G+g}{\sqrt{(G+g)^2+D^2}} + R - 1 \right], \tag{1}$$

and $R = M_{sx}/M_s$,

where M_{sx} is a saturated magnetization of the rod material. If both poles and rods are of the same material, $R=1$. Then the ΔB_1 on the lefthand side of Eq. (1) becomes ΔB_2 and is expressed by Eq. (2)

$$\Delta B_2(g) = \mu_0 M_s \left[\frac{G}{\sqrt{G^2+D^2}} - \frac{G+g}{\sqrt{(G+g)^2+D^2}} \right]. \tag{2}$$

In Eq. (1) and Eq. (2) the rod length is assumed to be infinite. If it is finite, the ΔB value has the form of $\Delta B_3(g, l)$ and is

$$\Delta B_3(g, l)=\mu_0 M_s\left[\frac{G}{\sqrt{G^2+D^2}}+R\frac{G+g+2l}{\sqrt{(G+g+2l)^2+D^2}}-R\frac{G+g}{\sqrt{(G+g)^2+D^2}}-1\right]. \quad (3)$$

The radial variation of magnetic field ΔB_4 can also be estimated as in Eq. (4) by applying the uniformly magnetic-charged disk approximation. (see Fig. 3)

$$\Delta B_4(x, g, G, D)=2[f(x, G/2, D)-f(x, G/2+g/2, D)], \quad (4)$$

where

$$f(x, A, G)=\int_0^{D/2} dr\int_0^{2\pi} d\varphi\frac{A}{t^3}r\frac{\mu_0 M_s}{4\pi}. \quad (5)$$

This integral contains a third kind of elliptic integral. The value f was evaluated with a numerical integration.

The effective field perturbation on an ion orbit in the cyclotron has the value of

$$<\Delta B\cdot L>=\int\Delta B\cdot dL, \quad (6)$$

where ΔB is the variation of the field along the orbit path L. To evaluate Eq. (6), a linear part from $-\infty$ to $+\infty$ is used. *i.e.,*

$$<\Delta B\cdot L>=\int_{-\infty}^{\infty}\Delta B\,dx$$

The effect of a pair of disks (see Fig. 3) is

$$<B\cdot L>=\frac{\mu_0 M_s}{2}\int_0^{D/2} dr\int_0^{2\pi} d\varphi\int_{-\infty}^{\infty}\frac{A\cdot r}{t^3}dx=\frac{\mu_0 M_s}{2}(\sqrt{D^2+G^2}-G). \quad (7)$$

Applying (7) to the system in Fig. 2, the $<\Delta B\cdot L>$ becomes

$$<\Delta B\cdot L>=\frac{\mu_0 M_s}{2}\left(\sqrt{D^2+\left(\frac{G}{2}+h\right)^2}-2\sqrt{D^2+\left(\frac{G}{2}+\frac{h}{2}\right)^2}+\sqrt{D^2+\left(\frac{G}{2}\right)^2}\right), \quad (8)$$

if $h/2$ is the rod length and also the rod position.

Eq. (2) and Eq. (4) were compared with the measured values. Eq. (8) is used to evaluate the range of field variation which could be covered by trim rods.

III. EXPERIMENT

To study the effect of trim rods, it is necessary to measure the field distribution where the ferromagnetic material is saturated. Nickel saturates at only 0.6T and makes the experiments easy. A test magnet as shown in Fig. 4 was constructed. The

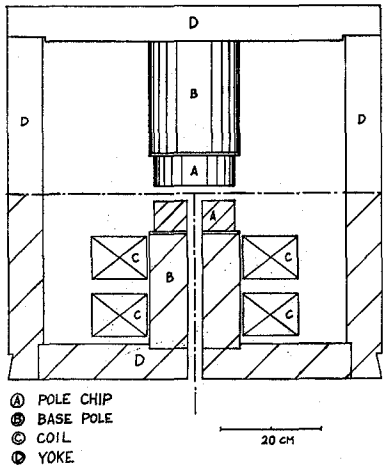

Fig. 4. Test magnet with trim rod.

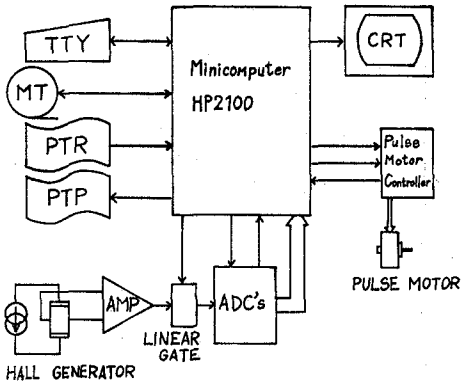

Fig. 5. Block diagram of the measuring system.

yokes and the base pole are made of iron. On the base pole, a pole chip of Nickel of 6 cm thickness was fixed by screws.

The block diagram of the measuring system is shown in Fig. 5. A Hall generator in a temperature regulated box[2] was used as a magnetic field measuring device and was moved by a pulse motor. The system was controled by a minicomputer of which program was written in FORTRAN and ASSEMBLER. The program was written to make the communication with the computer possible. The Hall generator output signal, which was calibrated in the uniform field of a large magnet with an NMR method, was converted into 13 bits digital number and was stored in the minicomputer. The measured data are displayed on a CRT in the form of field distribution, and output onto a MT. The accuracy of field measurement is in the order of 5 Gauss.

IV. RESULTS

Figure 6 shows the magnetic field distribution with a fixed exciting current where the rod position was varied in several steps of rod displacement. The distribution at four levels of exciting current are shown in Fig. 7.

The maximum perturbation along the axial line of the rod according to each rod position is shown in Figs. 8–a to 8–c. The "TRIM" values are calculated with the computer code TRIM. The "Equation" values are of Eq. (2), and the "Experiment" values are the results obtained with the test magnet.

The radial variation is also shown in Fig. 9. The "Numerical Integration" values are of Eq. (4).

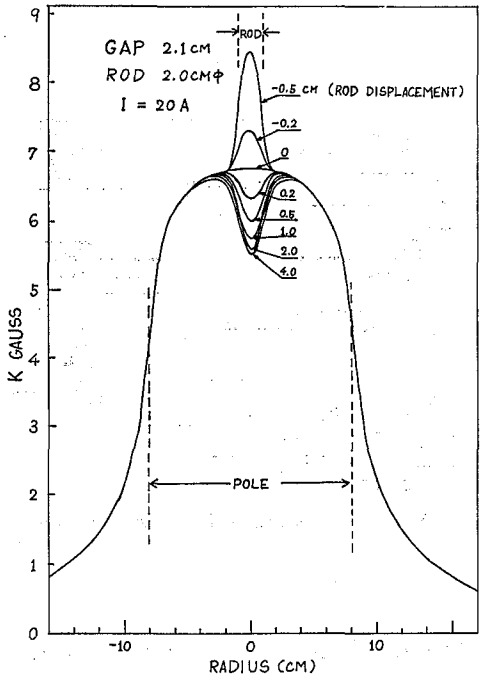

Fig. 6. Radial magnetic field variation corresponding to several positions of trim rod.

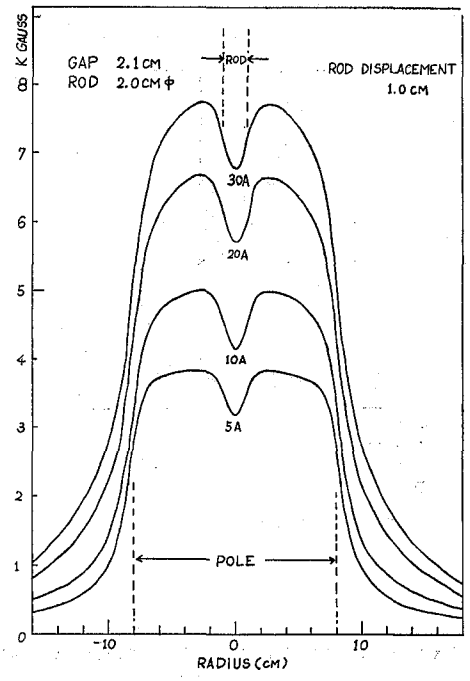

Fig. 7. Radial magnetic field distribution corresponding to several levels of exciting current.

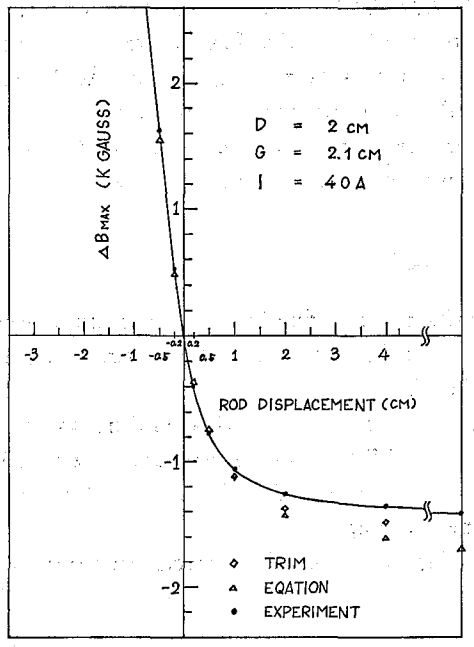

Fig. 8 a.

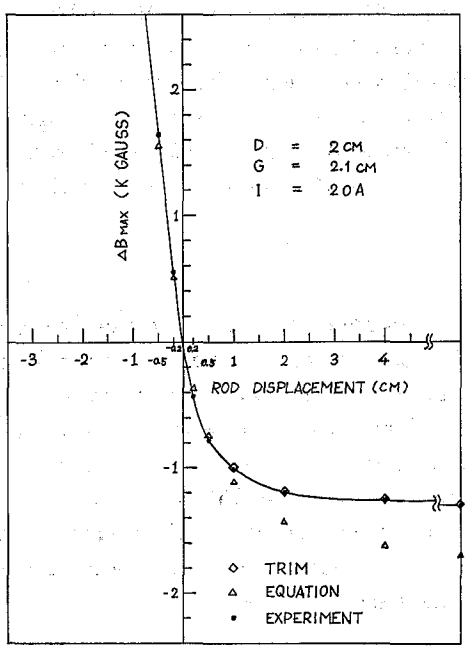

Fig. 8 b.

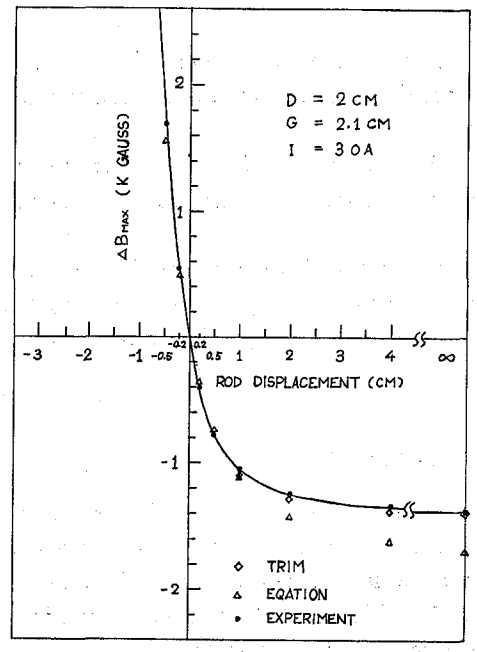

Fig. 8 c.

Fig. 8. Maximum magnetic field perturbation *vs* rod position for $D=2$ cm and $G=2.1$ cm, (a) 40A exciting current, (b) 30A exciting current, (c) 20A exciting current.

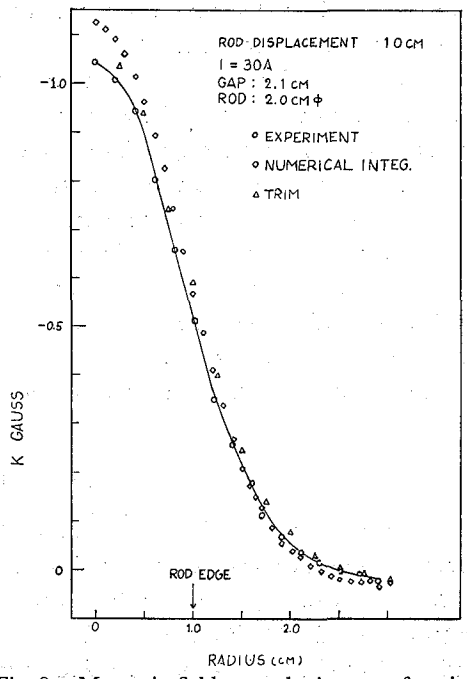

Fig. 9. Magnetic field perturbation as a function of distance from the center line of trim rod along the median plane. Solid line is only a guide for the eye.

V. DISCUSSION

The uniform magnetization approximation is practical for fields of supersaturation

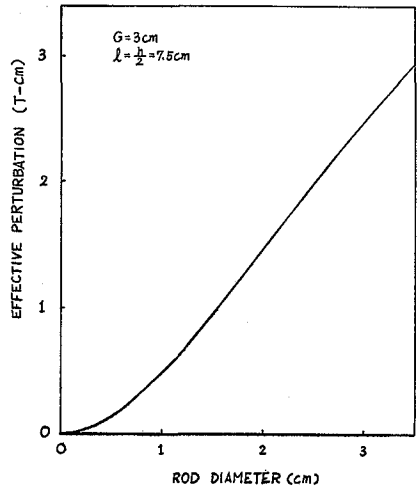

Fig. 10. Effective perturbation of magnetic field given by Eq. (8). Rod length and displacement is 7.5 cm. Rod gap is 3 cm.

level. Just above the saturation, the measured perturbations are appreciably smaller than theoretical prediction.

As seen in Fig. 8, the effect of the rod does not increase so much when the rod displacement exceeds one diameter length. Therefore, the rod should be used at some displacement of less than one diameter length.

The effective perturbation given by Eq. (8) is shown in Fig. 10. Because the uniform magnetization approximation is verified practical, one can use this equation to design the arrangement of trim rods.

Suppose a cyclotron of three sectors with a mean field 5T and suppose the necessary field perturbation is in the order of 1% of the mean field strength, that is usually the case of heavy ion acceleration, the field perturbation of 1[T-cm] at 10 cm radius is required. This value is achievable by the use of trim rods as seen in Fig. 10.

ACKNOWLEDGMENTS

The authors would like to thank Prof. T. Yanabu and Prof. H. Takekoshi for their continuous encouragements through the present work. They are also grateful to Mr. T. Miyanaga and Mr. S. Kizaki for their aids to perform this work, and are indebted to Mr. M. Yamada for Eqs. (5) and (7). The TRIM calculation was done with FACOM M190 at the Data Processing Center, Kyoto University.

APPENDIX

For reference, the triangular mesh and associated flux lines calculated by TRIM are shown in Figs. A–1 and A–2. The calculation is made under a cylindrical symmetry condition. Therefore, the apparent flux density in Fig. A–2 does not indicate the field strength. Figure B shows a CRT display of information on magnetic field measurement.

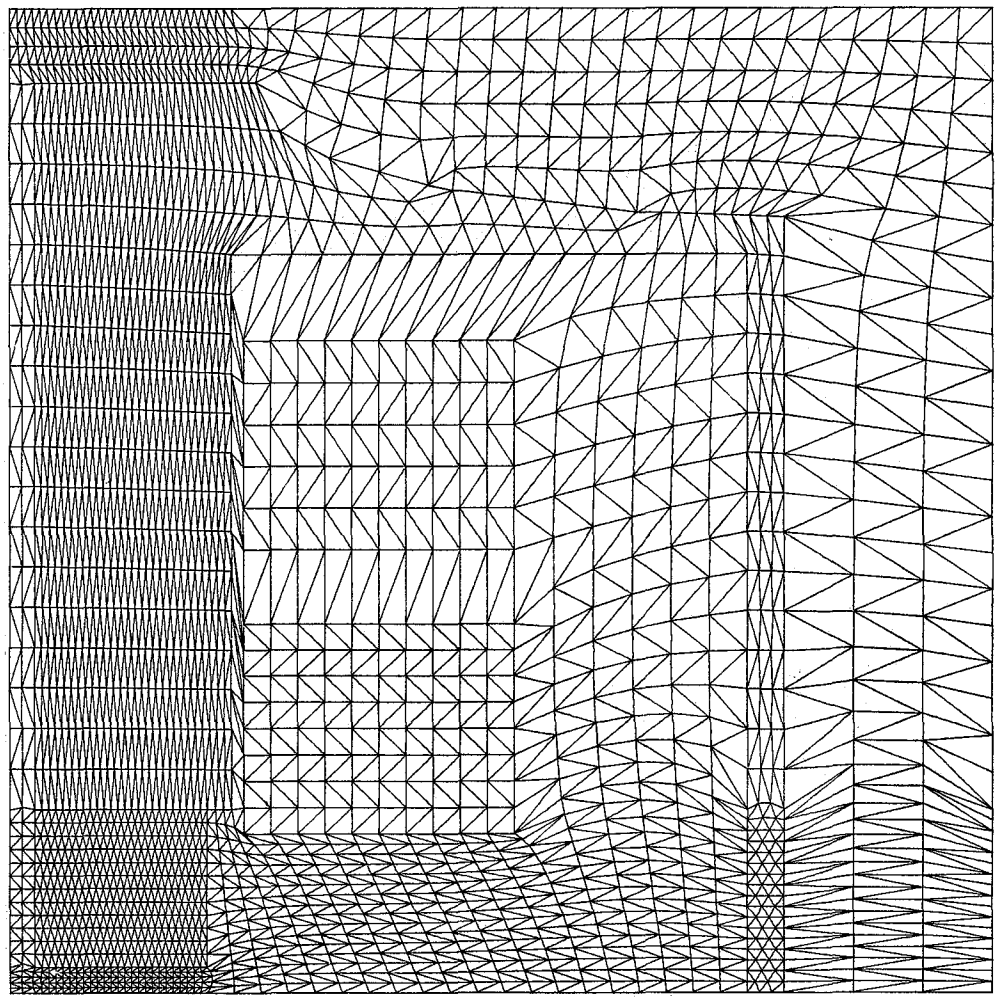

Fig. A–1

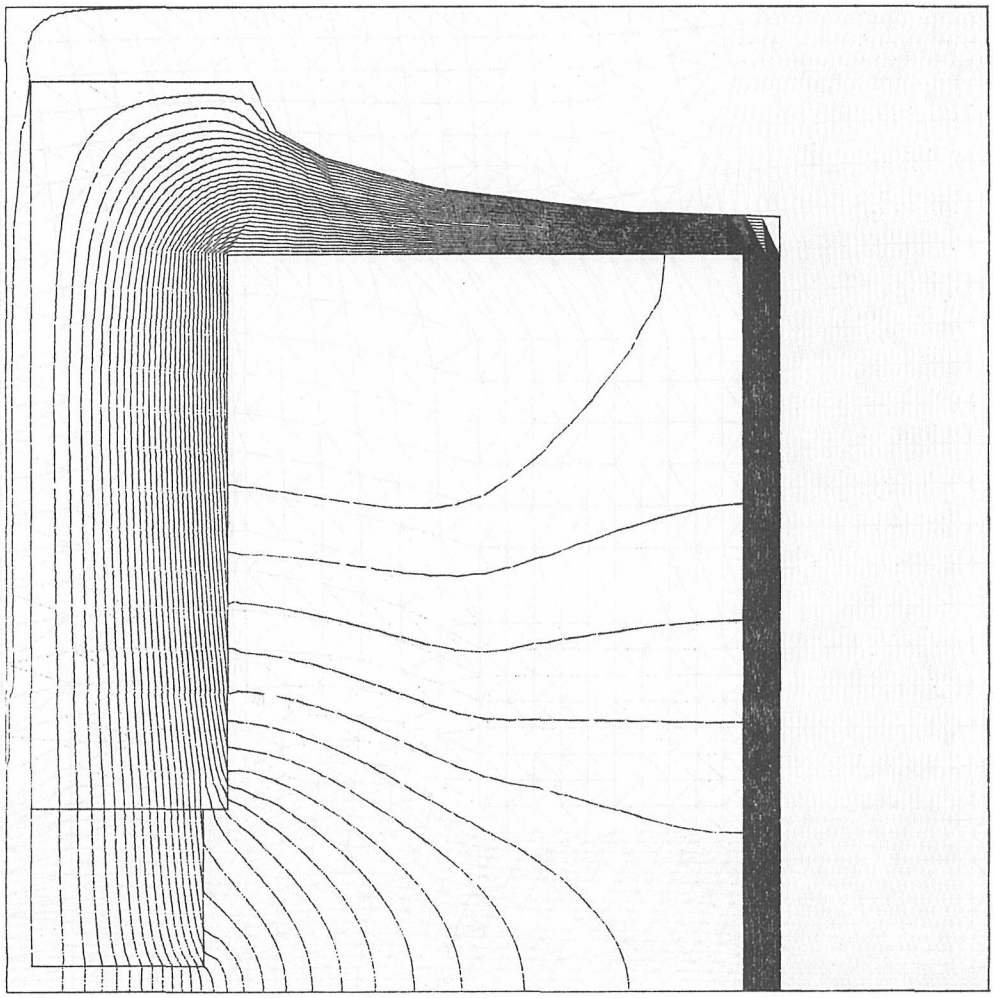

Fig. A–2

Fig. A. Example of TRIM.
(1) triangular mesh, (2) flux lines.

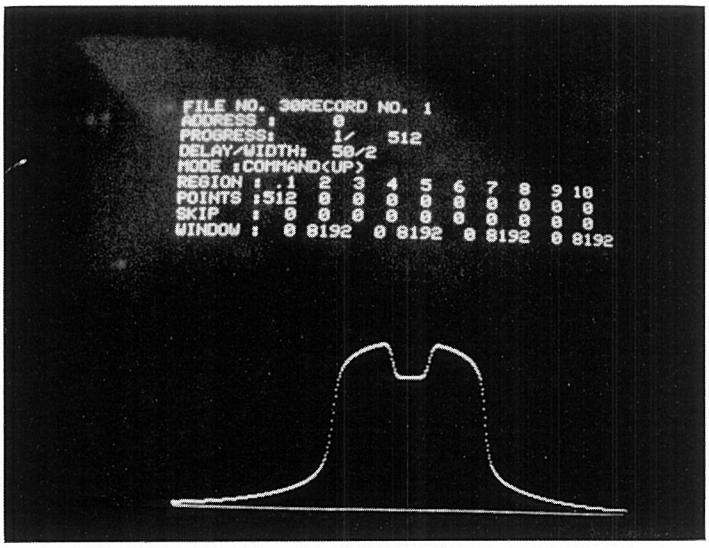

Fig. B. CRT display of information on magnetic field measurement.

REFERENCES

(1) C. B. Bigham, *Nucl. Instr.* & *Meth.* **131**, 223 (1975).
(2) E. D. Hudson, *Nucl. Instr.* & *Meth.* **18–19**, 159 (1962).